Nanostructure of Cationic Lipid-Oligonucleotide Complexes

Sarah Weisman,* Danielle Hirsch-Lerner,† Yechezkel Barenholz,† and Yeshayahu Talmon*
*Department of Chemical Engineering, Technion-Israel Institute of Technology, Haifa 32000, Israel; and †Department of Biochemistry, Hebrew University-Hadassah Medical School, Jerusalem 91120, Israel

ABSTRACT Complexes (lipoplexes) between cationic liposomes and single-strand oligodeoxynucleotides (ODN) are potential delivery systems for antisense therapy. The nanometer-scale morphology of these assemblies is relevant to their transfection efficiency. In this work the monocationic lipid dioleoyloxytrimethylammoniumpropane, the neutral "helper" lipid cholesterol, and an 18-mer anti-bcl2 ODN were combined at different ratios. The lipoplexes formed were characterized for the quantity of ODN bound, for the degree of lipid mixing, and for their size. The nanostructure of the system was examined by cryogenic-temperature transmission electron microscopy, augmented by small-angle x-ray scattering. Addition of ODN to cationic liposomes induced both liposome aggregation and the formation of a novel condensed lamellar phase. This phase is proposed to be stabilized by anionic single-strand ODN molecules intercalated between cationic bilayers. The proportion of cholesterol present apparently did not affect the nature of lipoplex microstructure, but changed the interlamellar spacing.

INTRODUCTION

Antisense oligodeoxynucleotides (ODN) are short single-strand DNA molecules designed to specifically hybridize to mRNA within a cell, inhibiting expression of the corresponding proteins (Leamon et al., 2003). ODN are useful tools for study of gene function, and also have many potential therapeutic applications, targeting proteins involved in disease. Despite some concerns about ODN selectivity (Lebedeva and Stein, 2001), one antisense drug has received FDA approval, and many others are in clinical trials (Flaherty et al., 2001; Tamm et al., 2001). A serious limitation to the success of antisense therapy is the inefficient cellular uptake of naked ODN (Akhtar, 1998). Transfection efficiency can be improved by use of a delivery system, such as complexes between ODN and cationic lipids, known as lipoplexes (Bennett et al., 1992).

Lipoplexes are formed spontaneously when cationic liposomes, which often also include a neutral ''helper'' lipid, are mixed with nucleic acids such as DNA, RNA, and ODN. The complexes are believed to protect nucleic acids from degradation, to enhance cellular uptake by endocytosis, and to facilitate release from the endosomal compartment (Dass, 2002; Zelphati and Szoka, 1997). Although extensive research has been done on the characterization of DNA-based lipoplexes (Dass, 2002), only a few studies have investigated the structure and physicochemical properties of ODN lipoplexes (Jääskeläinen et al., 1998; Meidan et al., 2000). Also, the similarities and differences between DNA and ODN lipoplexes are not clear. Better understanding of structure and physicochemical properties is a prerequisite for rational design of optimal ODN lipoplexes for in vitro and in vivo applications.

This study aimed to characterize the nanostructure of a cationic lipid-ODN system by direct nanoscale imaging (cryogenic transmission electron microscopy), augmented by quantitative measurements (small-angle x-ray scattering). Lipoplexes were composed of various ratios of the monocationic lipid N-(1-(2,3-dioleoyloxy)propyl),N,N,N-trimethylammonium chloride (DOTAP), the neutral ''helper'' lipid cholesterol, and the 18 mer G3139 phosphorothioate ODN. DOTAP/cholesterol lipid formulations have high efficacy in DNA transfection in vivo (Templeton et al., 1997; Dass, 2002; Simberg et al., 2003). ODN G3139 targets the bcl-2 gene, an apoptosis inhibitor, and is currently in clinical trials as a treatment for a variety of tumors (Flaherty et al., 2001; Tamm et al., 2001).

MATERIALS AND METHODS

Materials

Carboxyfluorescein-PE (CFPE) and lissamine rhodamine-PE (LRPE) for fluorescence experiments were purchased from Avanti Polar Lipids (Alabaster, AL). The monocationic lipid DOTAP was also obtained from Avanti Polar Lipids. Cholesterol (Chol), a neutral lipid, was purchased from Sigma (St. Louis, MO). The antisense 18-mer phosphorothioate ODN G3139 [S-d-5′-(TCT CCC AGC GTG CGC CAT)] was kindly donated by Genta (Lexington, MA). ODN purity was assessed by high-performance liquid chromatography (Merck Hitachi D-7000, Darmstadt, Germany), using an anion exchange column, and a single sharp peak was obtained. Liposomes were prepared by mixing *tert*-butanol solutions of DOTAP and cholesterol to mole ratios 1:0, 4:1, 2:1, or 1:1. The mixtures were freeze-dried overnight, then the lyophilized ''cakes'' were hydrated with 20 mM Hepes buffer at pH 7.4. Liposome suspensions were combined with concentrated ODN solution in buffer to give $ODN^-/DOTAP^+$ lipoplex charge ratios of 0, 0.2, 0.33, 0.5, 1, or 2.

Submitted August 17, 2003, and accepted for publication March 18, 2004.

Address reprint requests to Yeshayahu Talmon, Dept. of Chemical Engineering, Technion-Israel Institute of Technology, Haifa 32000, Israel. E-mail: ishi@tx.technion.ac.il.

0006-3495/04/07/609/06 $2.00

doi: 10.1529/biophysj.103.033480

Cryogenic transmission electron microscopy (cryo-TEM)

Liposomes and lipoplexes of charge ratio <1 were prepared at total lipid concentration of 2.5 mM as above, and vitrified shortly after addition of ODN to limit aggregate size. Lipoplexes of charge ratio ≥ 1 were prepared at total lipid concentration 1 mM, and sonicated by microtip at ~40 W power for 1.5 min before vitrification, to break up large aggregates. A control sample vitrified at a range of times (~30 s to ~30 min) after mixture of ODN with lipid, with or without sonication, showed no significant changes in morphology except varying aggregate size. Specimens were prepared in a controlled environment vitrification system at 25°C and 100% relative humidity, as previously described (Bellare et al., 1988; Danino et al., 2001). Samples were examined in a Philips CM120 microscope (Eindhoven, The Netherlands) operated at 120 kV, using an Oxford CT-3500 cooling holder and transfer station (Abingdon, England). Specimens were equilibrated in the microscope below −178°C, then examined in the low-dose imaging mode to minimize electron beam radiation damage, and recorded at a nominal underfocus of 2–4 μm to enhance phase contrast. Images were acquired digitally by a Gatan MultiScan 791 cooled charge-coupled device camera (Pleasanton, CA) using the Digital Micrograph 3.1 software package. Measurements of lamellar spacing by cryo-TEM are averages over at least 50 individual lamellae.

Small-angle x-ray scattering

Lipoplexes of selected $ODN^-/DOTAP^+$ charge ratios were prepared at total lipid concentration 2.5 mM as above, then centrifuged at ~1000 × *g* for 5 min. Pellets were redispersed in small quantities of the supernatants, then the suspensions were placed in 2-mm diameter sample capillaries. Small-angle x-ray scattering (SAXS) measurements were performed at 25°C in one of two facilities, either a sealed tube x-ray generator (Philips PW1730, Cu anode, Almelo, The Netherlands) with a compact Kratky camera (A. Paar, Graz, Austria) and a linear position-sensitive detector (Raytech, Paris, France), or a sealed tube x-ray generator (Kristalloflex K760-80, Cu anode, Bruker, Karlsruhe, Germany) with cross-coupled Göbel mirrors, a high-resolution x-ray small-angle pinhole chamber (A. Paar), and a two-dimensional multiwire area detector (Bruker). Data were collected over an 18-h period, and each system was assayed several times.

Fluorescence resonance energy transfer

The fluorescent probes (CFPE and/or LRPE) were mixed with DOTAP in *tert*-butanol at a probe/lipid mole ratio of 1:200. The mixtures were freeze-dried overnight, then hydrated in 20 mM Hepes buffer (pH 7.4) to 1 mM lipid concentration. ODN was added to a −/+ charge ratio of 0.5, and ~5 min were allowed for lipoplex formation. The spectra of the fluorescently labeled liposomes and lipoplexes were measured by a Perkin Elmer Life Sciences LS50B spectrofluorometer (Norwalk, CT) at excitation wavelength of 480 nm and emission wavelength of 515–600 nm. The efficiency of energy transfer (*E*) was calculated (Lakowicz, 1999) for each system.

Determination of bound ODN

Lipoplex suspensions were prepared at a total lipid concentration of 1 mM as above. After ~10 min for lipoplex formation the suspensions were centrifuged at 21,000 × *g* for 40 min at room temperature. The supernatant was removed. The pellet was dissolved in 20 μl of 20% sodium dodecyl sulfate and vortexed, then diluted with buffer. The distribution of ODN (the only molecule containing phosphorus in this system) between lipoplexes and solution was determined from the quantities of organic phosphorus in the supernatant and in the pellet, using the modified Bartlett method (Barenholz and Amselem, 1993).

Light scattering

Liposomes and lipoplex suspensions were prepared at a total lipid concentration of 1 mM as above. After ~10 min for lipoplex formation, dynamic light scattering (DLS) experiments were performed using an ALV-NIBS/HPPS particle sizer with an ALV-5000/EPP multiple digital correlator (ALV-Laser Vertriebsgesellschaft GmbH, Langen, Germany). Right-angle static light scattering (SLS) measurements were performed on a Perkin-Elmer LS 50B luminescence spectrometer (Norwalk, CT) with a 1 cm light path cell, using excitation and emission wavelengths of 600 nm, over a period of 10 s.

RESULTS

Direct imaging of nanostructure

Cryo-TEM examination of thin films of vitrified samples showed that lipid suspensions, at all cholesterol ratios, contained solely liposomes. The liposomes were unilamellar or oligolamellar, and heterogenous in shape and size. Fig. 1 *A* shows a representative vitrified oligolamellar liposome, with well-defined concentric bilayers. The two layers of each bilayer are clearly resolved. In lipid formulations containing >50 mol % cholesterol, excess cholesterol was found to separate and precipitate as microcrystals (not shown).

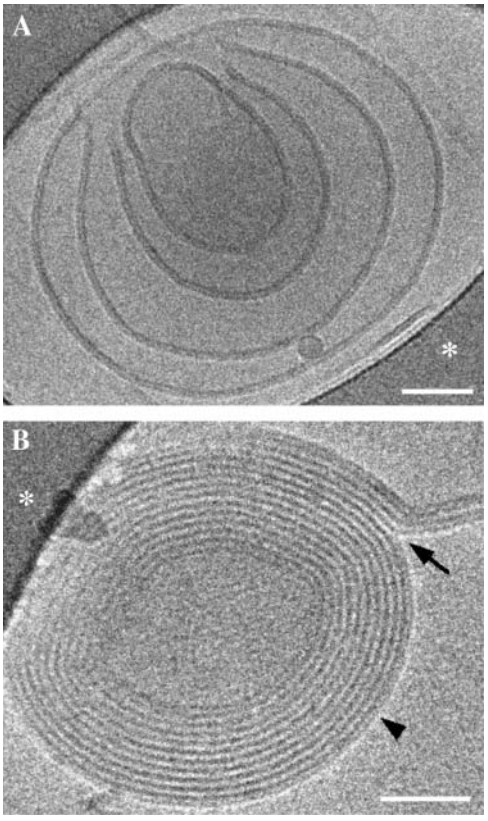

FIGURE 1 Cryo-TEM images showing the effect of ODN addition to cationic liposomes. (*A*) An oligolamellar liposome composed of DOTAP/Chol 4:1. (*B*) A complex of DOTAP/Chol 4:1 with ODN, at ODN/lipid charge ratio 0.33. Lipid membranes are seen fusing (*arrow*) to a condensed multilamellar particle (*arrowhead*). Asterisks mark areas of supporting carbon film. Scale bars represent 50 nm.

Addition of ODN to lipid suspensions, regardless of cholesterol ratio, caused aggregation of most liposomes into larger complexes. At an excess of lipid, several types of nanostructure were observed within the complexes, as shown in the main panel of Fig. 2. Liposomes or liposomal membranes (*double arrows*) coexisted with novel assemblies resembling three ''triplet'' parallel lines (*white arrowheads*) and dense multilayered particles (*black arrow*).

The initially puzzling triplet structures (Fig. 2, *upper inset*) were demonstrated to consist of two liposomal membranes adsorbed to one another (Fig. 2, *lower inset*). Note that each triplet consists of a thick dark central line and thinner outer lines (*white arrows*). Black arrowheads indicate points where bilayers join to form triplets.

The multilayered particles were found to be composed of concentric lamellae, considerably more closely and evenly spaced than in a standard multilamellar liposome. Fig. 1 *B* shows bilayers in the process of fusing (*arrow*) to the outermost layer of a condensed multilamellar particle. Condensed particles frequently contained lamellar defects and/or incomplete outer bilayers, as shown in the inset of Fig. 3.

The local levels of condensation and aggregation of lipoplexes were observed to be heterogenous. However, increasing concentration of ODN, regardless of cholesterol ratio, increased the prevalence of the condensed lamellar particles, at the expense of discrete or paired membranes. Aggregate sizes also seemed to increase with ODN concentration, although cryo-TEM cannot accurately measure average size, as the largest structures may have been excluded from samples. At the isoelectric point and at excess ODN large aggregates of condensed multilamellar particles were the dominant microstructures; free liposomes were rare (Fig. 3).

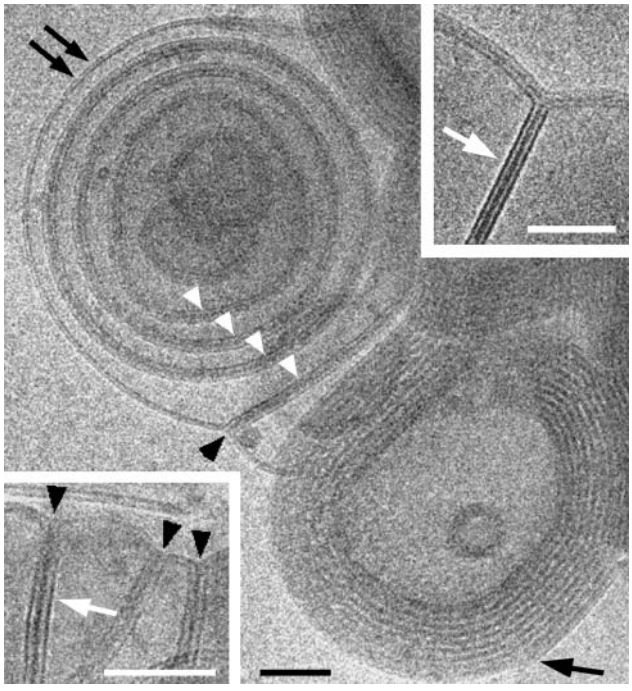

FIGURE 2 Cryo-TEM images of systems with excess lipid, showing the coexistence of several nanostructures. A lipoplex of DOTAP/Chol 1:1 with ODN/lipid charge ratio 0.2 contains discrete membranes (*double arrow*), paired membranes (*white arrowheads*), and condensed lamellar phase particles (*black arrow*). (*Upper inset*) DOTAP/Chol 1:1, charge ratio 0.33: a clearer image of paired membrane structures (*white arrow*). (*Lower inset*) DOTAP/Chol 2:1, charge ratio 0.2: adsorption of liposomes to each other to form paired membrane structures, with black arrowheads indicating membrane junctions and a white arrow pointing to a paired membrane. Scale bars represent 50 nm.

Measurement of nanostructure

SAXS experiments were performed to measure the interlamellar spacing of multilamellar particles for selected lipid-ODN formulations (Table 1). SAXS scattering curves (not shown) gave a well-defined first lamellar peak, but a broad and weak second lamellar peak (in some cases undetectable), suggesting short-range order. Interlamellar spacing was also measured with lower precision from cryo-TEM images (Table 1), and the two techniques produced consistent results.

Lipid mixing

Fluorescence resonance energy transfer experiments were performed to determine whether ODN induces intervesicle lipid mixing. Control DOTAP/CFPE/LRPE liposomes (containing both a fluorescence donor and an acceptor) had efficient energy transfer ($E = 0.760 \pm 0.003$). Addition of ODN slightly increased the energy transfer ($E = 0.785 \pm 0.002$), probably due to interactions between probes in adjacent condensed lamellae. When DOTAP/CFPE (donor only) and DOTAP/LRPE (acceptor only) liposomes were mixed, there was a very low level of energy transfer ($E = 0.025 \pm 0.022$). Addition of ODN caused a small increase in efficiency ($E = 0.089 \pm 0.037$), of the same order as seen in the control liposomes. This indicates that ODN does not induce significant lipid mixing in the short term.

ODN distribution

Phosphate assays determined the distribution of ODN between lipoplexes (found in the pellet of centrifuged samples) and solution (the supernatant). As shown in Fig. 4, for all lipid formulations, complexation of ODN was most efficient at $ODN^-/lipid^+$ charge ratios of 0.5 or 1. The greatest quantities of ODN were bound within lipoplexes at the isoelectric points. At a constant total lipid concentration, lipid membranes with higher DOTAP mole fraction (with higher charge) captured larger quantities of ODN.

Aggregate size

DLS experiments attempted to determine particle size distribution. The mass-weighted average size of liposomes,

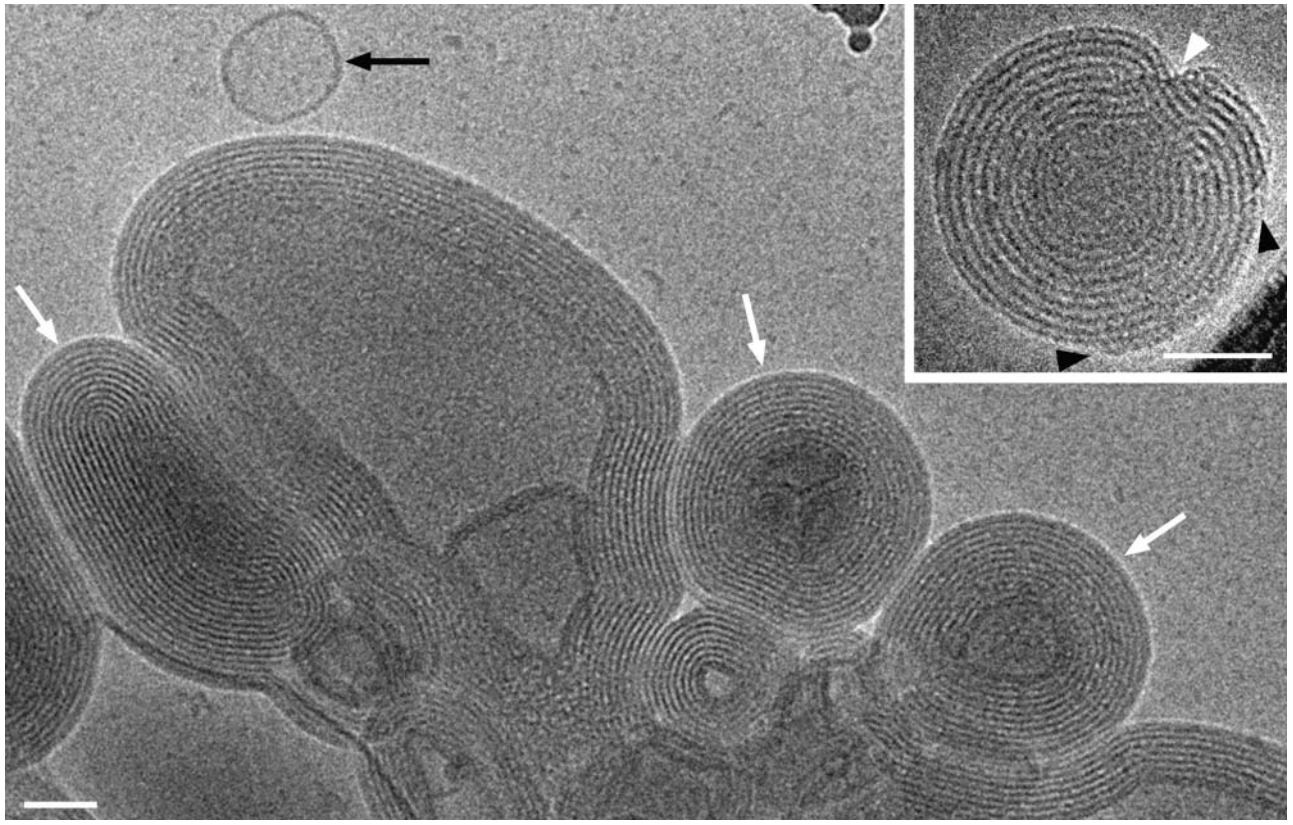

FIGURE 3 Cryo-TEM images showing developed lipid-ODN ordered phase. A lipoplex of DOTAP with ODN at the isoelectric point is an aggregation of condensed multilamellar particles (*white arrows*), coexisting with a few free liposomes (*black arrow*). (*Inset*) DOTAP/Chol 1:1, charge ratio 1: a condensed multilamellar particle at higher magnification. Black arrowheads indicate incomplete outer bilayers, whereas a white arrowhead marks a lamellar defect due to incomplete inner bilayers. Scale bars represent 50 nm.

regardless of their cholesterol ratio, was found to be ~700 ± 150 nm. Addition of ODN caused dramatic increases both in mean particle size and in particle size heterogeneity. The two parameters reached a maximum at $ODN^-/lipid^+$ charge ratios of 0.5 or 1. However the high degree of aggregate size heterogeneity, probably together with a strong dependence on sample preparation conditions, made the quantitative DLS measurements irreproducible.

Direct imaging of a single sample (DOTAP/Chol 2:1, charge ratio 0.5) ~5 min after mixture of ODN with liposomes showed aggregates ranging from smaller than 200 nm (by cryo-TEM) to larger than 4 μm (by Nomarski digital light microscopy). The concept of average size is not really relevant to a system with this degree of heterogeneity.

TABLE 1 Measurements of interlamellar distances in lipid-ODN systems by SAXS and by cryo-TEM

Lipid formulation	ODN/lipid charge ratio	d-spacing (nm) SAXS	d-spacing (nm) TEM
DOTAP	0.5	4.9 ± 0.2	4.9 ± 0.5
DOTAP/Chol 4:1	0.5	5.3 ± 0.2	5.0 ± 0.5
DOTAP/Chol 2:1	0.5	5.2 ± 0.2	4.7 ± 0.5
DOTAP/Chol 1:1	0.5	5.7 ± 0.2	5.1 ± 0.5
DOTAP/Chol 1:1	2	5.3 ± 0.2	5.4 ± 0.5

Right-angle static light scattering experiments provided a rough gauge of the level of vesicle aggregation. The turbidity of lipoplex dispersions (T) was measured in relation to the turbidity of their parent lipid suspensions (T_0) (Table 2). For all lipid formulations, lipoplex aggregation apparently increased with ODN concentration, peaking at $ODN^-/lipid^+$ charge ratios of 1 or 2, in agreement with the findings

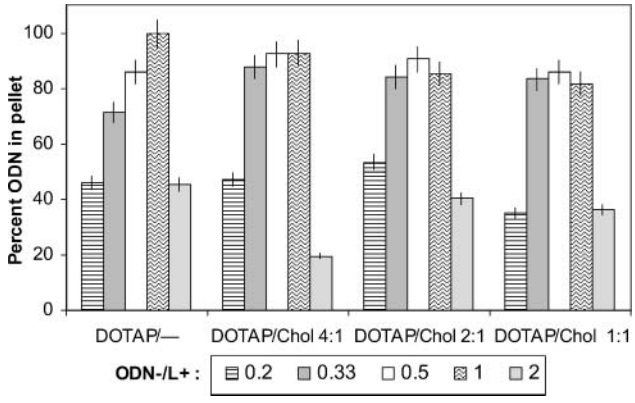

FIGURE 4 Percentage of ODN bound in lipoplexes as a function of ODN charge ratio for different lipid formulations, as determined by phosphate assays.

TABLE 2 Turbidity of lipid-ODN systems ~10 min after mixing

	ODN^-/L^+					
Lipid formulation	0	0.2	0.33	0.5	1	2
DOTAP	1	2.36	3.48	4.34	5.04	7.48
DOTAP/Chol 4:1	1	1.89	2.18	3.70	6.76	6.51
DOTAP/Chol 2:1	1	1.55	1.82	3.12	3.95	4.17
DOTAP/Chol 1:1	1	1.30	1.56	2.56	2.93	2.56

Data are presented as T/T_0, where T is the 90° SLS measurement of the lipoplex sample, and T_0 is the 90° SLS measurement of the parent lipid suspension.

of other techniques. As the cholesterol content of the lipoplex formulations increased, the turbidity decreased for all charge ratios.

DISCUSSION

Mixing ODN with cationic liposomes induces liposome aggregation and lamellar condensation. Single-strand ODN molecules cannot be directly observed by cryo-TEM; however, their location may be inferred from their effect on larger structures. Cationic membranes are observed adsorbing to each other to form paired membranes (Fig. 2, *black arrowheads*). This would normally be barred by electrostatic repulsions, but could be explained by oppositely charged ODN molecules acting as bridges between the membranes. Close examination of cryo-TEM images of paired membranes (Fig. 2, *insets*, *white arrows*) reveals that the plane of contact between bilayers has higher contrast than their outer edges, suggesting electron-dense ODN molecules sandwiched between the membranes. This phenomenon can also explain liposome aggregation, as ODN molecules could ''glue'' adjacent liposomes together.

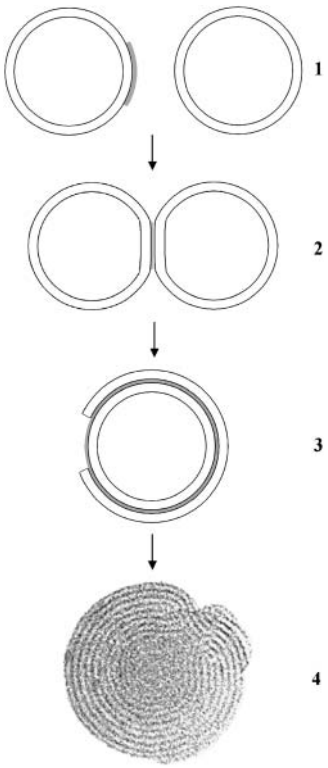

FIGURE 5 Schematic model of lipoplex formation. (*1*) Initially, anionic ODN molecules (*gray*) may coat a cationic membrane. (*2*) Two liposomes may adsorb to each other due to ODN bridging. This process causes liposome aggregation. (*3*) Destabilization due to partial charge neutralization may cause one membrane to rupture and wrap around another. (*4*) If local ODN concentration is sufficient, further membranes may adsorb to produce a condensed multilamellar particle (e.g., Fig. 3, *inset*) with intercalated ODN layers.

Condensed multilamellar particles have lamellar spacing very similar to the distance between paired membranes, and their outermost edge, as in paired membranes, has lower contrast than inner layers (Fig. 1 *B*, *black arrowhead*). This strongly suggests that the condensed lamellar phase is also stabilized by ODN bridges between cationic membranes. Condensed lamellar particles probably initiate from concentric paired membranes, then grow by ODN-mediated adsorption of additional membranes one by one (Fig. 1 *B*, *black arrow*). This would explain the frequent appearance of lamellar defects and incomplete outermost lamellae (Fig. 3, *inset*). Our suggested mechanism of lipoplex formation is illustrated in Fig. 5.

At higher concentrations of ODN, the growth of condensed lamellar particles may be limited by a scarcity of unbound membranes. Instead, ODN molecules may form bridges between the outermost membranes of neighboring particles, causing aggregation into large expanses of ordered phase (Fig. 3).

The ODN lipoplex morphology that we observed has similarities to the well-known ''sandwich'' phase formed by some cationic lipid-DNA systems. Early cryo-TEM studies (Gustafsson et al., 1995) of DNA lipoplexes showed images of aggregated multilamellar particles, and x-ray diffraction analysis (Rädler et al., 1997) demonstrated that these structures were lamellar with intercalated DNA. Many features of our model for ODN lipoplex formation (Fig. 5) resemble a proposed mechanism of liposome reorganization in the presence of DNA (Huebner et al., 1999). However, in the case of ODN lipoplexes, the lack of lipid mixing indicates that intervesicle fusion is not a significant phenomenon.

SAXS measurements (Table 1) corroborated the lamellar nature of the lipoplexes. We propose that the condensed lamellar structures are composed of alternating layers of cationic lipid bilayers and hydrated ODN. The interlamellar spacing of the DOTAP/ODN system is 4.9 ± 0.2 nm, and DOTAP bilayer thickness has been reported as 3.72 ± 0.03 nm (Rädler et al., 1998), consistent with our cryo-TEM observations. We therefore find that the aqueous layer thickness is 1.18 ± 0.23 nm, sufficient for a monolayer of ODN molecules. This can be compared with the DOTAP/DNA lamellar phase, where the DNA layer thickness was

found to be significantly larger, ~2.3 nm (Rädler et al., 1998). The difference is mainly due to the greater diameter of the double-strand DNA helix, and probably also greater hydration of DNA. In addition, as ODN is single-strand and lacks defined secondary structure, possibly some side groups of the ODN chain can penetrate into the head group region of the bilayers, an impossibility for rigidly structured DNA helices. Another distinction between the two lamellar phases is that neither cryo-TEM nor SAXS detected any ordering of the intercalated ODN molecules, whereas DNA forms a monolayer lattice of parallel helices. Indeed, we would expect the short, flexible ODN molecules to orient fairly randomly between the membranes.

Addition of cholesterol seemed to have no qualitative effect on system nanostructure, but did alter the interlamellar spacing (Table 1). The general trend of expanding spacing with rising cholesterol ratio could be explained by two possible mechanisms. First, the rigid cholesterol molecule is known to increase the order parameter of phospholipid molecules in a bilayer (Jedlovszky and Mezei, 2003), straightening lipid hydrocarbon tails, and thus increasing bilayer thickness. This effect, however, is thought to be only weakly dependent on cholesterol concentration. Second, at high cholesterol ratios (50 mol %) cationic membranes are less densely charged (Meidan et al., 2000), and may bind ODN less closely, swelling the ODN layer between membranes. The loose binding may be reversed in conditions of excess ODN. Other effects of the presence of cholesterol in lipid bilayers are to lower the quantity of ODN associated with the lipoplexes (Fig. 4), and to decrease the turbidity of dispersions (Table 2), suggesting a lower level of aggregation. In addition, cholesterol may affect the dynamics of lipoplex formation or the stability of lipoplexes in various media such as serum, as was observed for DNA lipoplexes (Simberg et al., 2003).

Cationic lipid-ODN complexes, with a high density of ODN molecules intercalated and protected between lipid membranes, may be an effective delivery system for antisense therapy. Better understanding of the morphology and mechanism of aggregation of these systems is important for rational development of applications. Future studies should investigate nanostructure in conditions modelling an in vivo environment, and should attempt to identify structure-function relations.

We thank Dr. R. Khalfin and Prof. Y. Cohen for assistance with the SAXS measurements, and Genta Inc. for the generous gift of G3139 ODN.

This research was supported in part by grants from the Technion V.P.R. Fund to Y.T., the Canada–Israel Industrial Research and Development Foundation (CIIRDF) to Y.B., and the Israel Science Foundation to Y.T. and Y.B. jointly.

REFERENCES

Akhtar, S. 1998. Antisense technology: selection and delivery of optimally acting antisense oligonucleotides. *J. Drug Target.* 5:225–234.

Barenholz, Y., and S. Amselem. 1993. Liposome preparation and related techniques. *In* Liposome Technology, Vol. 1. G. Gregoriadis, editor. CRC Press, Boca Raton, FL. 527–616.

Bellare, J. R., H. T. Davis, L. E. Scriven, and Y. Talmon. 1988. Controlled environment vitrification system: an improved sample preparation technique. *J. Electron Microsc. Tech.* 10:87–111.

Bennett, C. F., M. Y. Chiang, H. Chan, J. E. Shoemaker, and C. K. Mirabelli. 1992. Cationic lipids enhance cellular uptake and activity of phosphorothioate antisense oligonucleotides. *Mol. Pharmacol.* 41:1023–1033.

Danino, D., A. Bernheim-Groswasser, and Y. Talmon. 2001. Digital cryogenic transmission electron microscopy: an advanced tool for direct imaging of complex fluids. *Colloid. Surface. A.* 183–185:113–122.

Dass, C. R. 2002. Biochemical and biophysical characteristics of lipoplexes pertinent to solid tumour gene therapy. *Int. J. Pharm.* 241:1–25.

Flaherty, K. T., J. P. Stevenson, and P. J. O'Dwyer. 2001. Antisense therapeutics: lessons from early clinical trials. *Curr. Opin. Oncol.* 13:499–505.

Gustafsson, J., G. Arvidson, G. Karlsson, and M. Almgren. 1995. Complexes between cationic liposomes and DNA visualized by cryo-TEM. *Biochim. Biophys. Acta.* 1235:305–312.

Huebner, S., B. J. Battersby, R. Grimm, and G. Cevc. 1999. Lipid-DNA complex formation: reorganization and rupture of lipid vesicles in the presence of DNA, as observed by cryoelectron microscopy. *Biophys. J.* 76:3158–3166.

Jääskeläinen, I., B. Sternberg, J. Mönkkönen, and A. Urtti. 1998. Physicochemical and morphological properties of complexes made of cationic liposomes and oligonucleotides. *Int. J. Pharm.* 167:191–203.

Jedlovszky, P., and M. Mezei. 2003. Effect of cholesterol on the properties of phospholipid membranes. 1: Structural features. *J. Phys. Chem. B.* 107:5311–5321.

Lakowicz, J. R. 1999. *In* Principles of Fluorescence Spectroscopy, 2nd ed. J. R. Lakowicz, editor. Kluwer Academic/Plenum Publishers, New York. 367–390.

Leamon, C. P., S. R. Cooper, and G. E. Hardee. 2003. Folate-liposome-mediated antisense oligodeoxynucleotide targeting to cancer cells: evaluation in vitro and in vivo. *Bioconjug. Chem.* 14:738–747.

Lebedeva, I., and C. A. Stein. 2001. Antisense oligonucleotides: promise and reality. *Annu. Rev. Pharmacol. Toxicol.* 41:403–419.

Meidan, V. M., J. S. Cohen, N. Amariglio, D. Hirsch-Lerner, and Y. Barenholz. 2000. Interaction of oligonucleotides with cationic lipids: the relationship between electrostatics, hydration and state of aggregation. *Biochim. Biophys. Acta.* 1464:251–261.

Rädler, J. O., I. Koltover, A. Jamieson, T. Salditt, and C. Safinya. 1998. Structure and interfacial aspects of self-assembled cationic lipid-DNA gene carrier complexes. *Langmuir.* 14:4272–4283.

Rädler, J. O., I. Koltover, T. Salditt, and C. R. Safinya. 1997. Structure of DNA-cationic liposome complexes: DNA intercalation in multilamellar membranes in distinct interhelical packing regimes. *Science.* 275: 810–814.

Simberg, D., S. Weisman, Y. Talmon, A. Faerman, T. Shoshani, and Y. Barenholz. 2003. The role of organ vascularization and lipoplex-serum immediate contact in intravenous murine lipofection. *J. Biol. Chem.* 278:39858–39865.

Tamm, I., B. Dörken, and G. Hartmann. 2001. Antisense therapy in oncology: new hope for an old idea? *Lancet.* 358:489–497.

Templeton, N. S., D. D. Lasic, P. M. Frederik, H. H. Strey, D. D. Roberts, and G. N. Pavlakis. 1997. Improved DNA: liposome complexes for increased systemic delivery and gene expression. *Nat. Biotechnol.* 15:647–652.

Zelphati, O., and F. C. Szoka. 1997. Cationic liposomes as an oligonucleotide carrier: mechanism of action. *J. Liposome Res.* 7:31–49.